Electronic Supplementary Material (ESI) for Journal of Materials Chemistry A.

Morphology of Cu Clusters Supported on Reconstructed Polar ZnO (0001) and $(000\bar{1})$ Surfaces

Michael D. Higham[a,b], David Mora-Fonz[c], Alexey A. Sokol[d], Scott Woodley[d], C. Richard A. Catlow[a,b,d]*

(a) *Research Complex at Harwell, Rutherford Appleton Laboratory, Harwell Oxford, Didcot, Oxon, OX11 0FA, UK.*
(b) *Cardiff University, School of Chemistry, Main Building, Park Place, Cardiff, CF10 3AT, UK.*
(c) *Department of Physics and Astronomy, University College London, Gower Street, London WC1E 6BT, UK.*
(d) *Kathleen Lonsdale Materials Chemistry, Department of Chemistry, University College London, 20 Gordon Street, London WC1H 0AJ, UK.*

* Corresponding author: highamm@cardiff.ac.uk

Supporting Information

Graphics are provided illustrating the structure of all of the low-energy structures for Cu clusters of various sizes on the four reconstructed ZnO surfaces discussed in the main text. All of these structures have been made publicly available via the SAINT database (https://saint.chem.ucl.ac.uk/). Additionally, a full discussion of the DFT refinement of the IP-obtained structures is provided.

Table S1: *Summary of the 5 lowest energy structures for various Cu cluster sizes over the O-terminated reconstructed ZnO surface featuring Zn adatoms.*

No. Cu Atoms	IP Rank				
	1	2	3	4	5
1	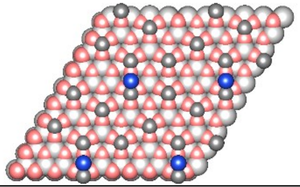	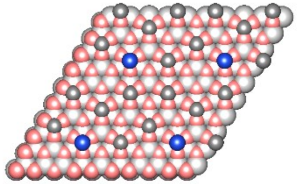	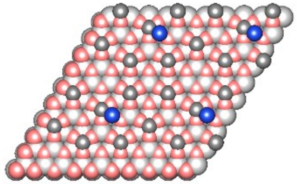	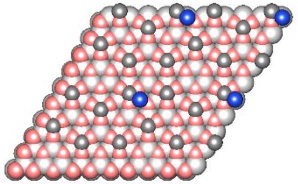	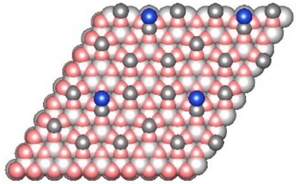
2	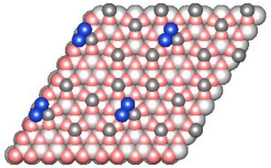	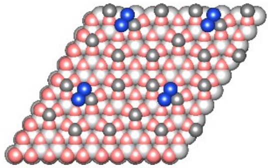	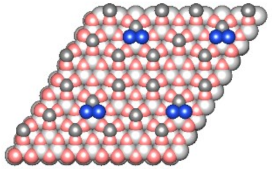	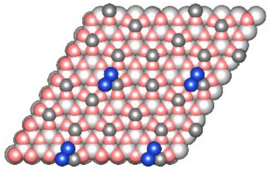	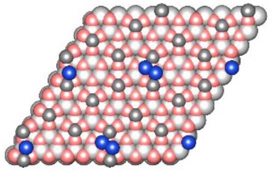
3	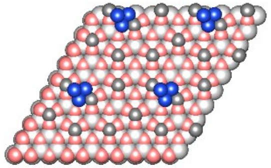	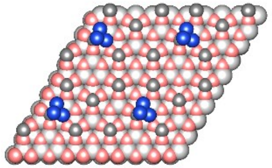	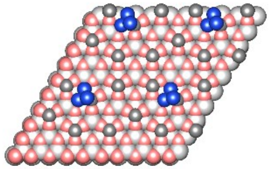	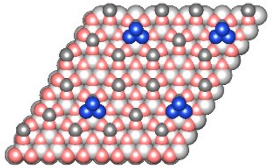	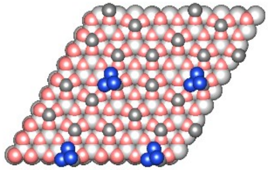
4	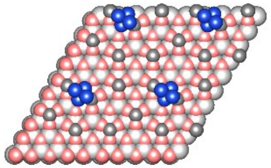	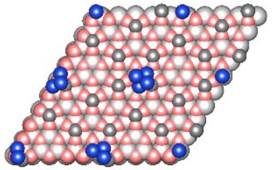	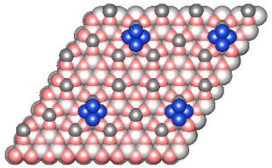	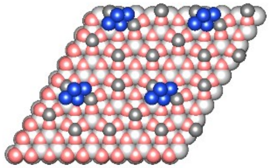	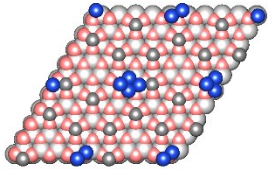
5	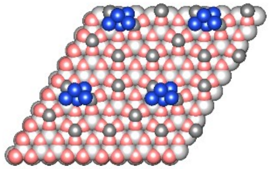	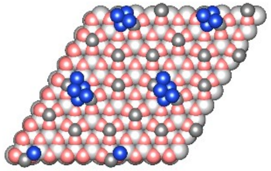	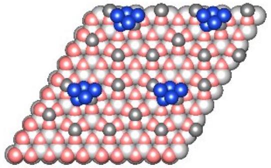	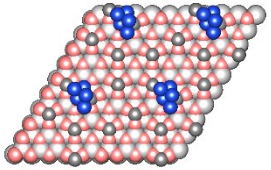	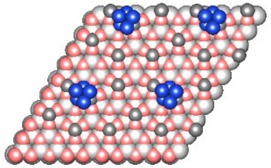

6	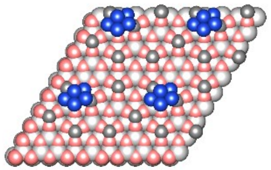	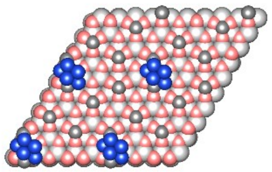	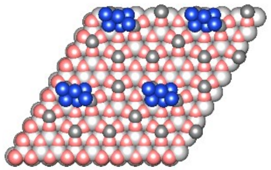	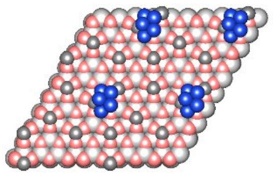	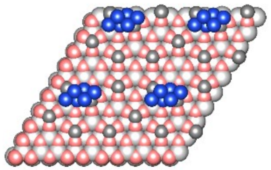
7	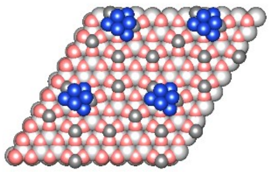	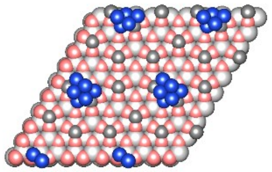	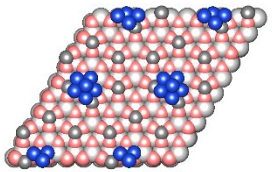	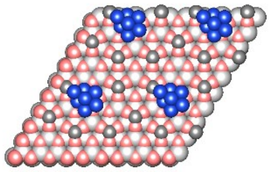	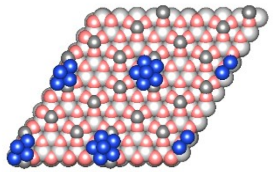
8	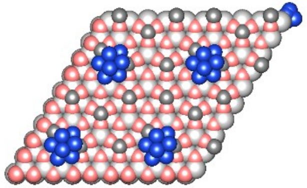	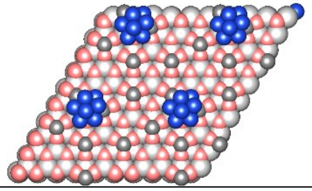	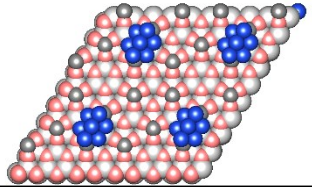	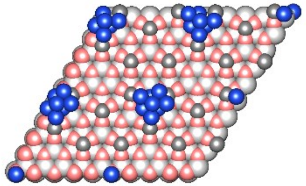	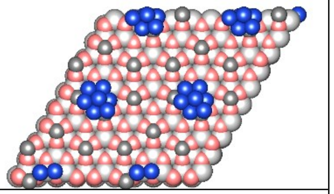
24	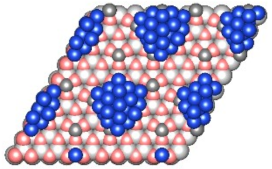	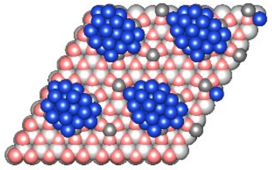	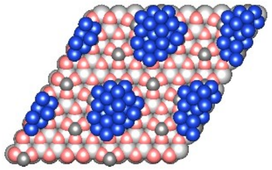	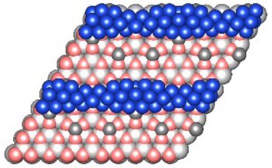	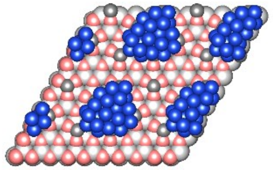
50	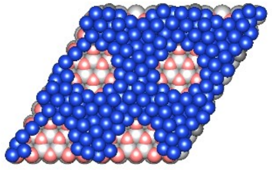	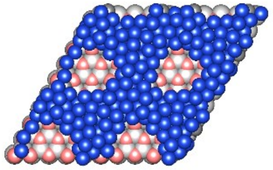	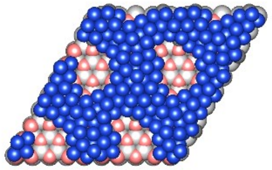	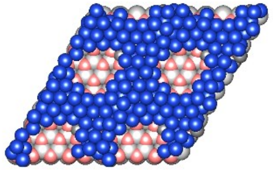	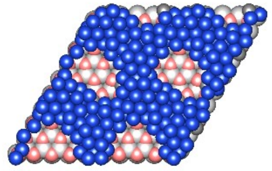

Table S2: *Summary of the 5 lowest energy structures for various Cu cluster sizes over the O-terminated reconstructed ZnO surface featuring O vacancies.*

No. Cu Atoms	IP Rank				
	1	2	3	4	5
1	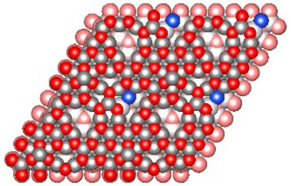	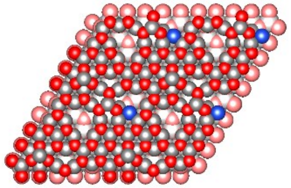	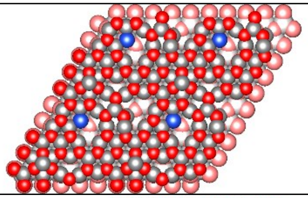	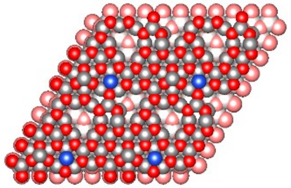	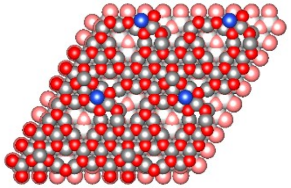
2	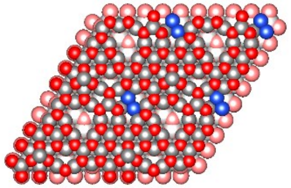	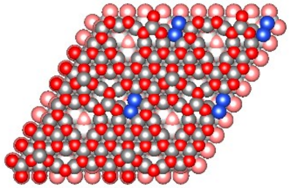	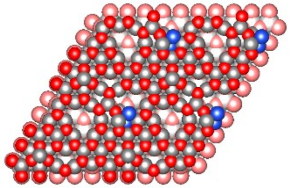	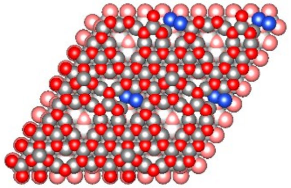	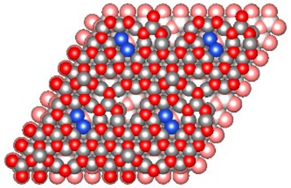
3	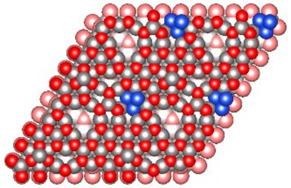	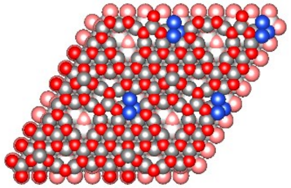	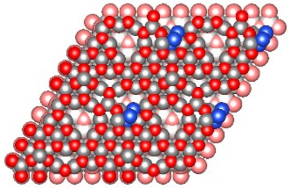	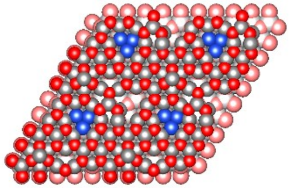	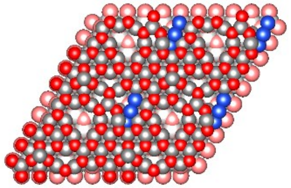
4	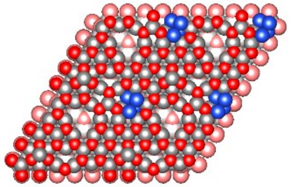	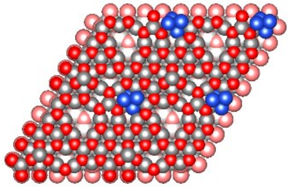	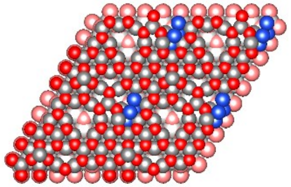	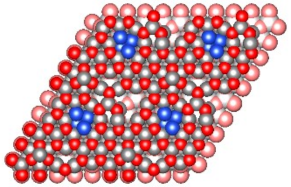	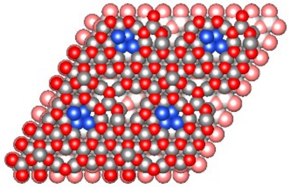
5	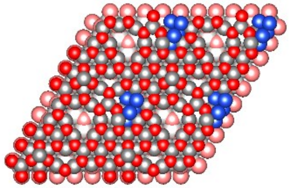	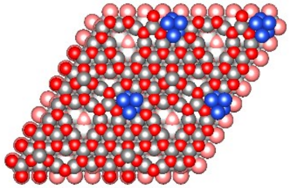	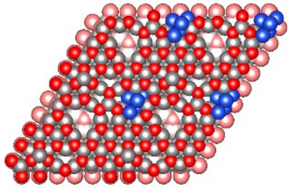	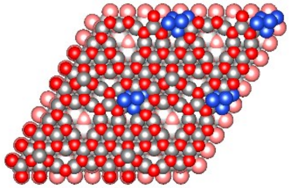	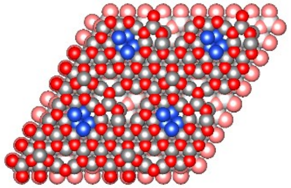

6	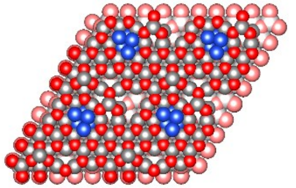	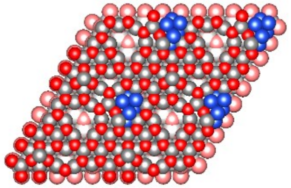	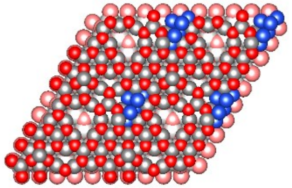	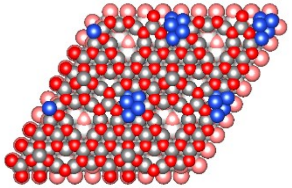	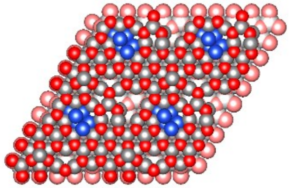
7	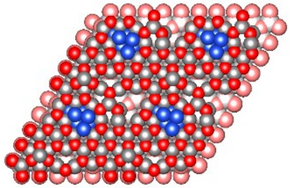	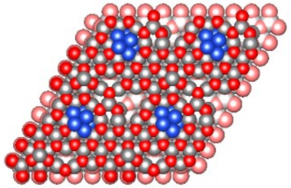	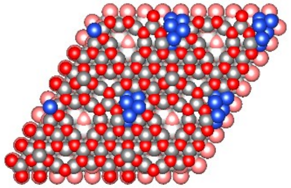	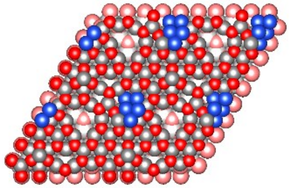	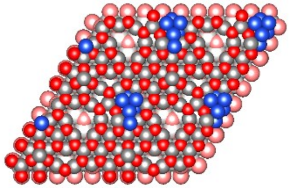
8	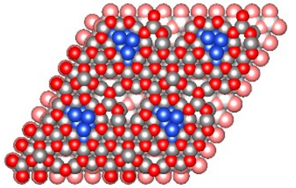	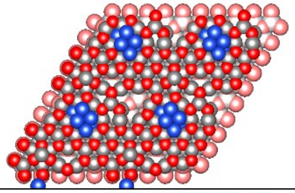	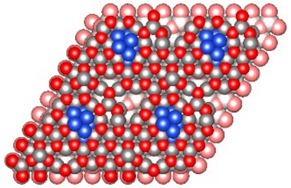	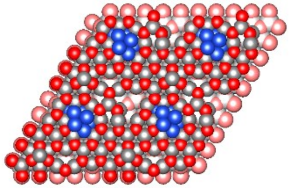	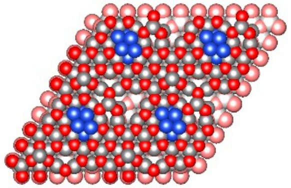
24	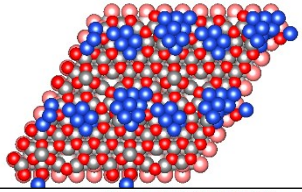	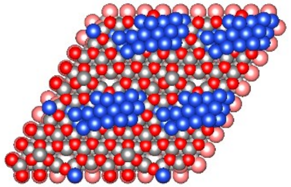	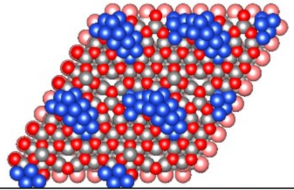	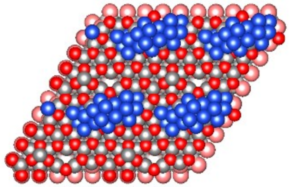	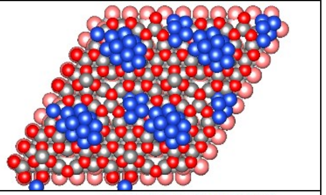
50	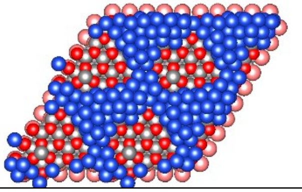	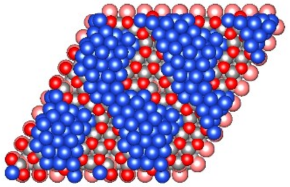	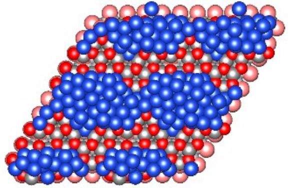	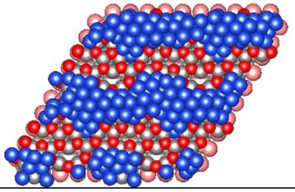	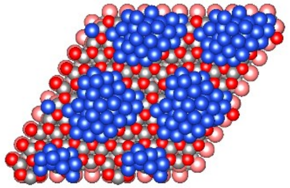

Table S3: *Summary of the 5 lowest energy structures for various Cu cluster sizes over the Zn-terminated reconstructed ZnO surface featuring O adatoms.*

No. Cu Atoms	IP Rank				
	1	2	3	4	5
1	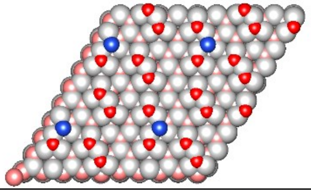	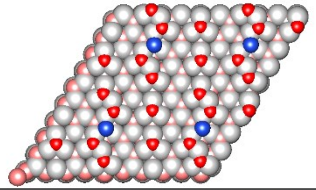	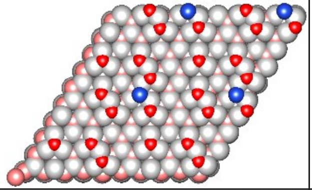	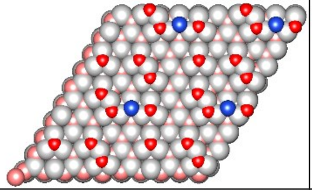	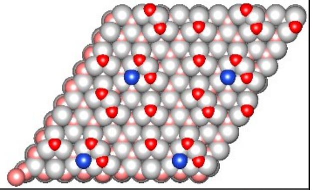
2	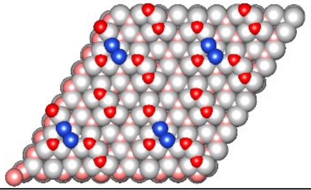	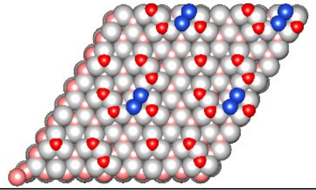	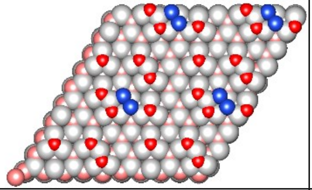	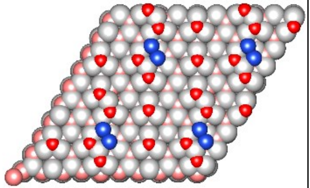	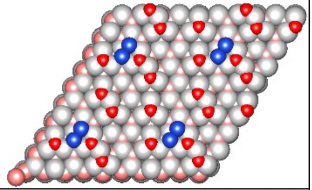
3	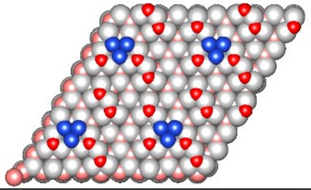	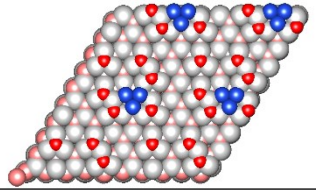	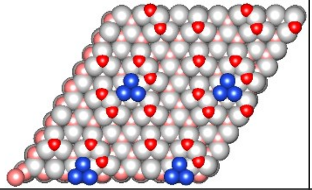	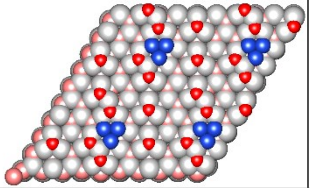	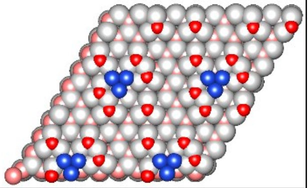
4	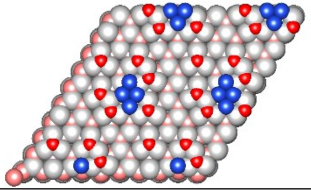	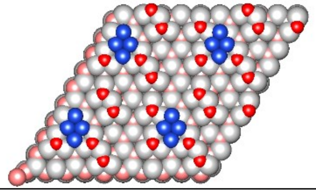	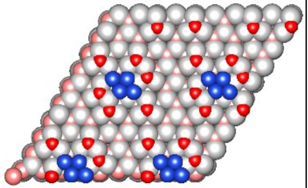	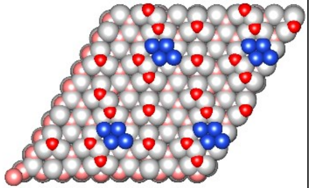	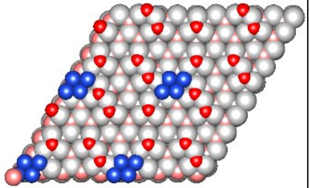
5	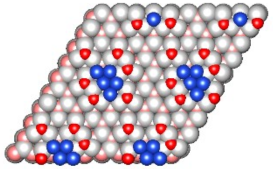	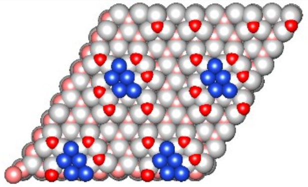	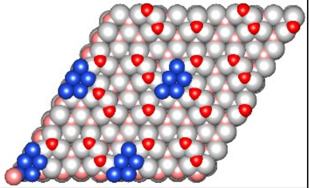	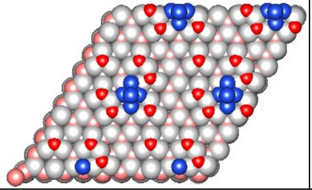	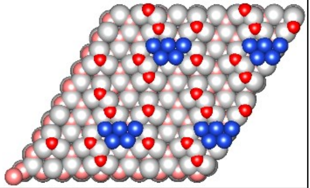

6	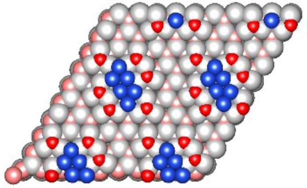	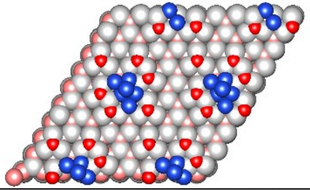	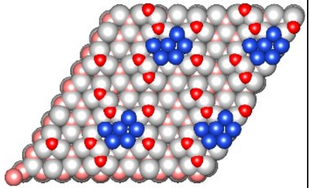	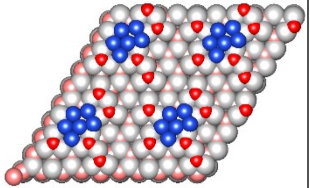	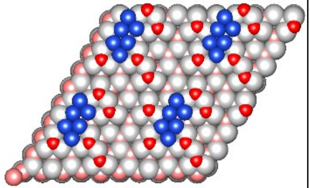
7	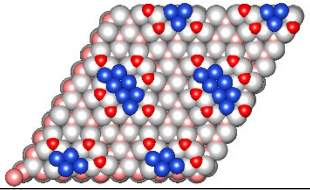	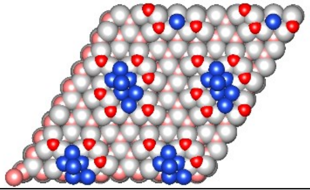	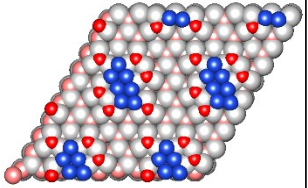	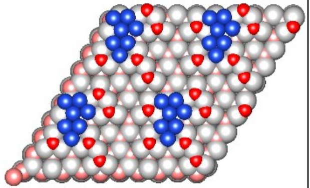	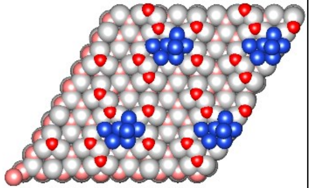
8	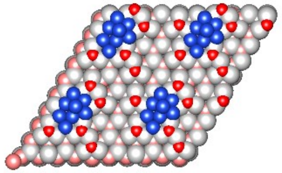	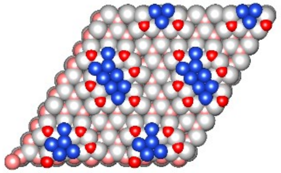	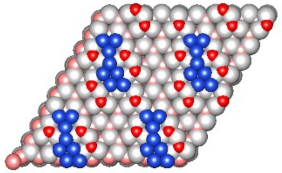	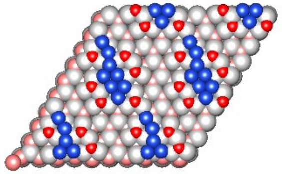	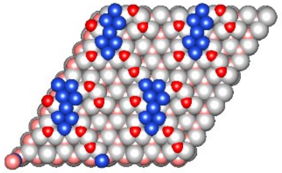
24	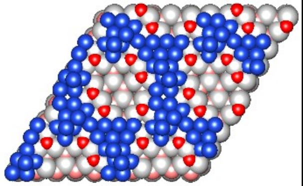	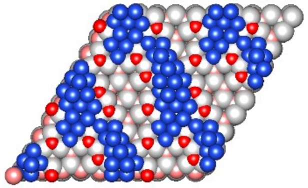	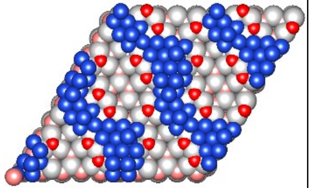	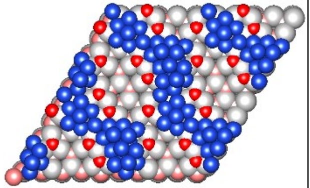	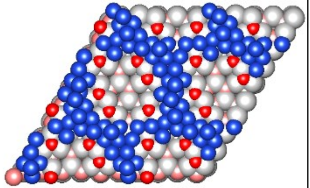
50	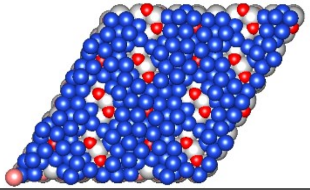	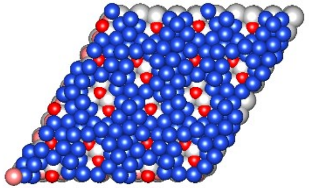	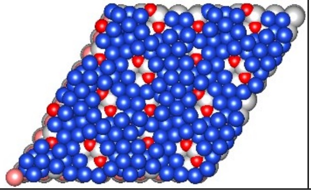	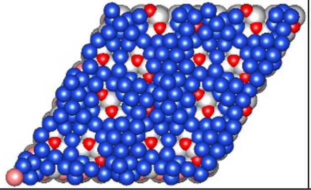	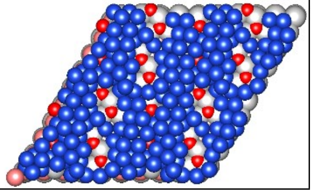

Table S4: *Summary of the 5 lowest energy structures for various Cu cluster sizes over the Zn-terminated reconstructed ZnO surface featuring Zn vacancies.*

No. Cu Atoms	IP Rank				
	1	2	3	4	5
1	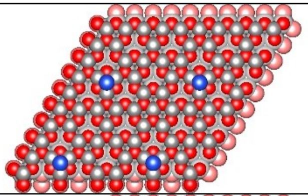	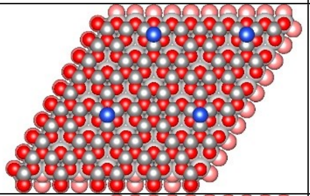	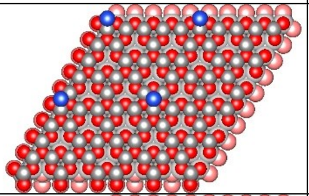	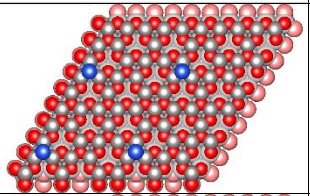	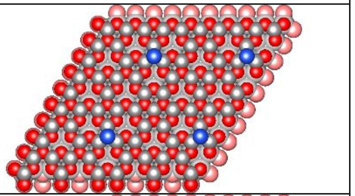
2	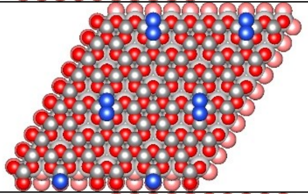	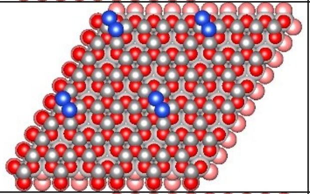	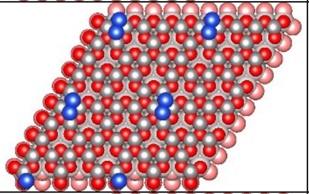	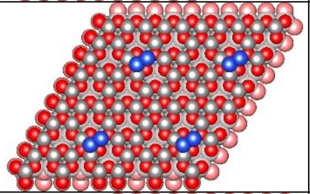	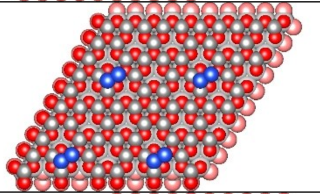
3	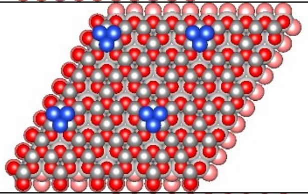	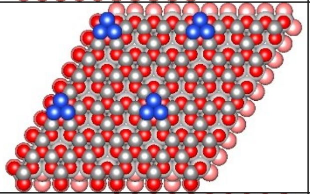	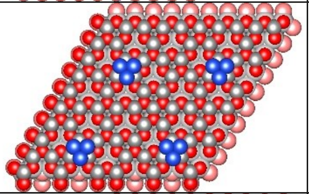	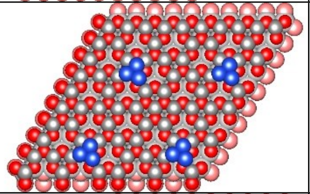	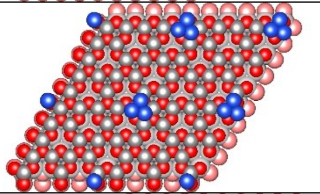
4	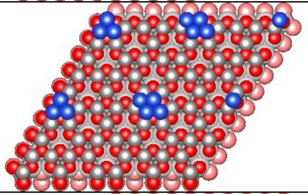	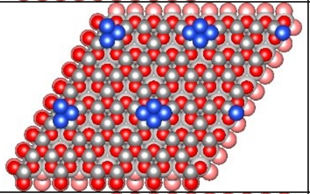	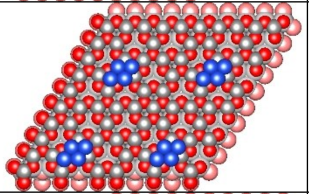	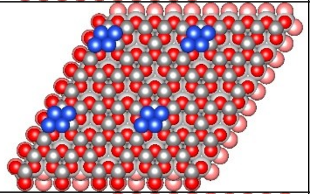	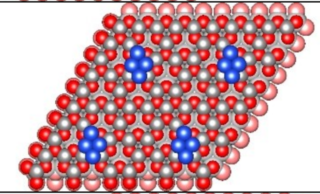
5	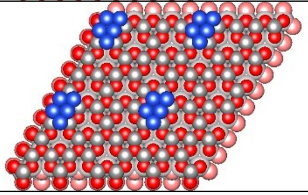	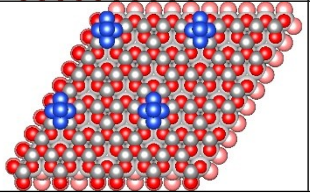	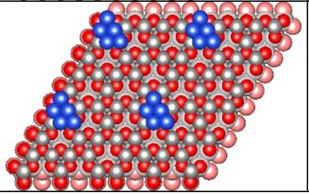	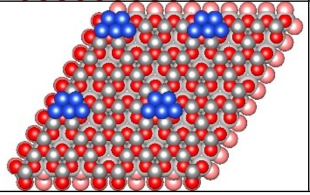	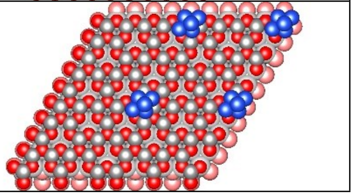

6	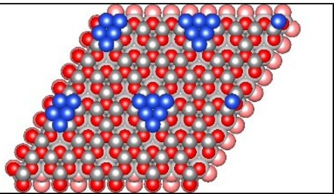	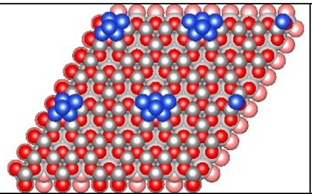	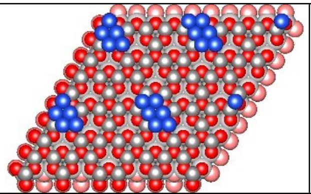	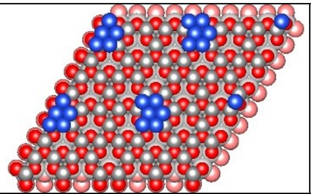	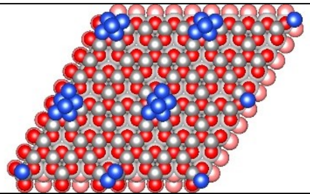
7	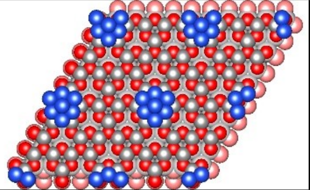	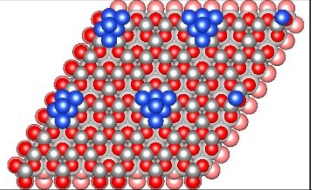	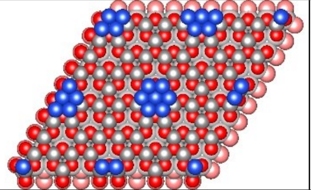	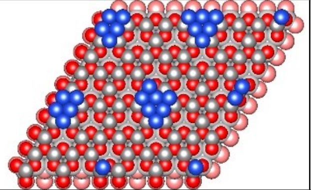	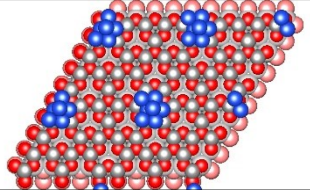
8	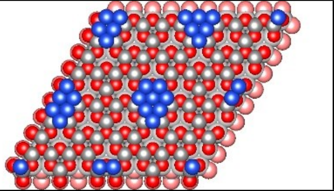	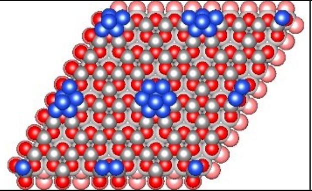	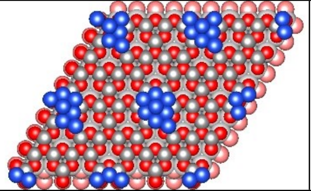	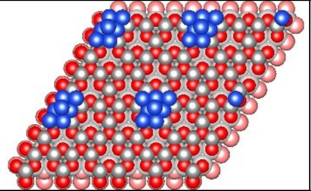	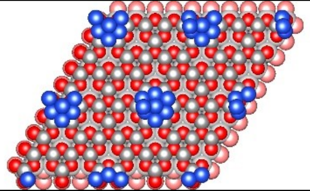
24	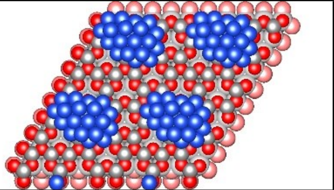	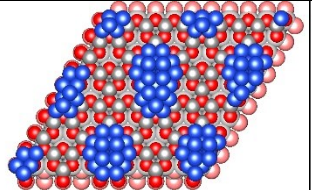	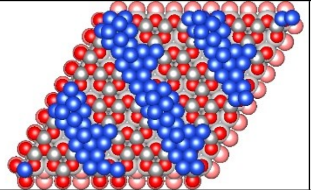	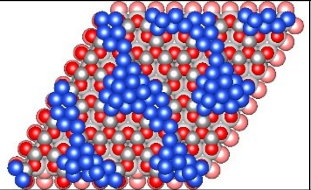	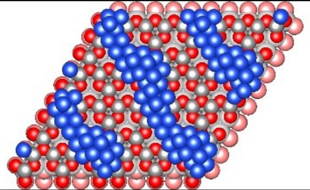
50	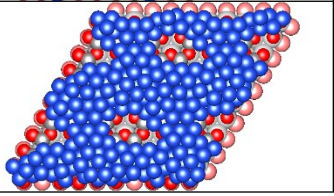	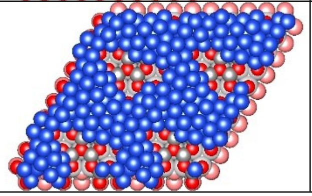	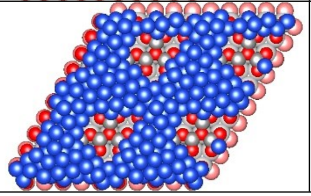	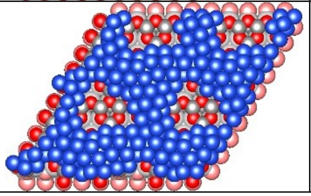	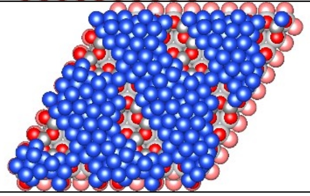

DFT Refinement of Cu_8 IP Structures

Having obtained structures for the five lowest energy IP structures for each of the surface reconstructions and a variety of Cu cluster sizes from the global optimisation studies, DFT refinement of these structures is required to verify the validity of the global optimisation approach, and to allow for a more detailed analysis. For this purpose, the Cu_8 clusters for each of the four surface reconstructions were subject to DFT refinement. Previous work investigating Cu cluster growth on the non-polar ZnO$(10\bar{1}0)$found that, overall, structural and energetic trends are well-reproduced between the two methods, indeed indicating that the IP global optimisation approach is suitable for screening large numbers of surface structural configurations without excessively compromising in terms of accuracy[16]. However, the reconstructed polar ZnO surface show a greater variety of surface features, namely the presence of Zn or O adatoms or vacancies, compared to the non-polar surface. Hence, it is of interest to consider whether the interatomic potentials accurately reproduce the interaction between the surface features and the Cu cluster, given that the highly undercoordinated surface atoms arising from the surface reconstruction may interact differently with Cu clusters compared to Zn and O atoms forming part of a complete, flat, surface ZnO layer, as in the case of the non-polar surface and unreconstructed polar ZnO surfaces.

Zn-rich O-terminated Surface

For Cu_8 clusters adsorbed on the Zn-rich O-terminated reconstructed surface (featuring Zn adatoms), an excellent agreement between the IP and DFT structures is observed for the top two lowest energy structures, with virtual identical Cu cluster geometries being obtained before and after DFT refinement (Table 9). Moreover, the overall trend in relative energy is well-reproduced, with the clear split in stability between the top two and remaining three structures being retained. However, there is some divergence in the IP and DFT relative energies for the

3rd, 4th and 5th lowest energy structures; using IP, all three of these configurations have a similar relative stability with respect to the global minimum, whereas after DFT refinement, we find that not only does the relative stability decrease with respect to the global minimum, but also that the stability ordering changes upon DFT refinement (with the 5th ranked IP structure being the 3rd ranked DFT structure), and that the range of relative stabilities between these three structures also increases after DFT refinement, increasing from 0.05 eV to 0.36 eV.

A possible explanation for the discrepancy between the very good agreement between the IP and DFT relative energies and structures for the top two lowest energy structures, and the more varied behaviour for the 3rd, 4th and 5th ranked structures, lies in the symmetry of the Cu cluster and its adsorption site. It can be seen that the Cu_8 cluster for the global minimum IP structure is identical to that of the 2nd lowest energy structure, differing only in its rotational orientation upon the ZnO surface, and that the cluster itself is highly symmetric compared to that of the 3rd, 4th and 5th ranked structures. Regardless of methodology, such symmetrical atomic arrangements necessarily mean an optimal degree of coordination; hence it is unsurprising that such structures appear as global minima and competing local minima using both IP and DFT methods. We also note that upon DFT optimisation, the surface Zn adatoms are more significantly displaced from their positions upon the clean reconstructed surface, which perhaps implies that whilst there is indeed a strong attractive interaction between Cu and Zn, for the highly undercoordinated Zn surface adatoms this interaction is somewhat overestimated using IP methods, since the Cu-ZnO potential fitting was performed by calibrating against a small Cu cluster interacting with a flat ZnO surface. Necessarily, such displacement of the Zn surface adatoms means a compromise in Zn-O coordination between the Zn adatoms and the subsurface O, resulting in these structures being more destabilised compared to the IP relative energies. The change in the ordering of the relative stabilities resulting from the 5th ranked IP structure being determined as the 3rd ranked DFT structure can be attributed to the fact that the IP structure undergoes the greatest extent of structural rearrangement of all of the five structures upon DFT optimisation, with the final DFT optimised structure closely resembling that of the global minimum, albeit with a much less symmetric Cu cluster geometry accounting for the ~0.6 eV difference in relative stability.

Table S5: *Structure and relative stability for the top 5 ranked low energy IP structures for Cu_8 clusters adsorbed on the reconstructed O-terminated ZnO surface featuring Zn adatoms, before and after DFT refinement.*

IP Rank	IP Structure	IP Relative E / eV	DFT Structure	DFT Relative E / eV
1	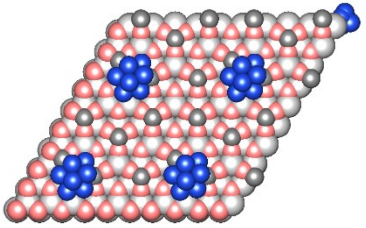	0.000000	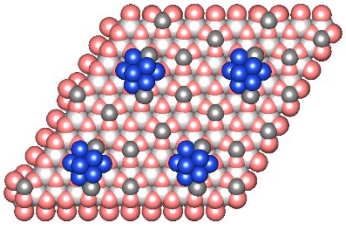	0.000000
2	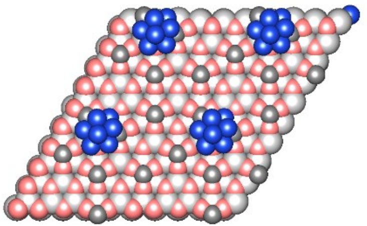	0.073720	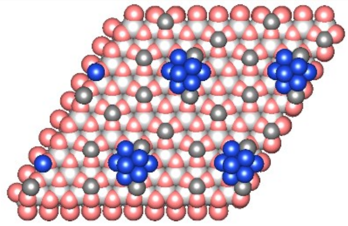	0.045052
3	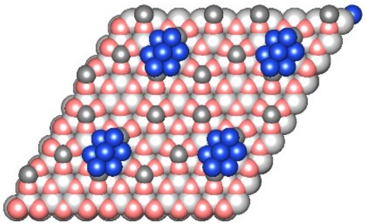	0.309003	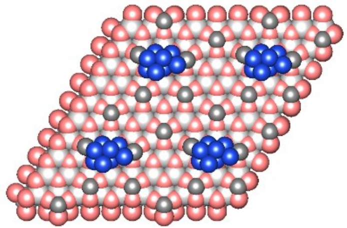	0.896847
4	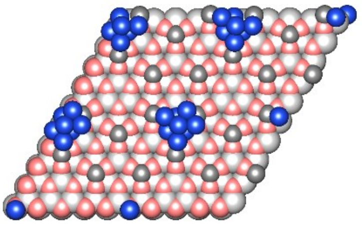	0.357594	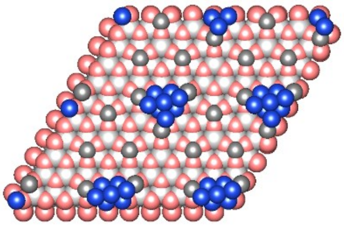	1.059009
5	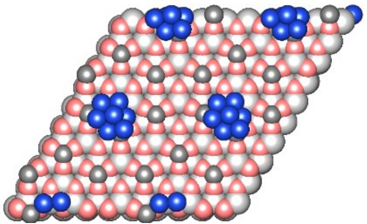	0.361627	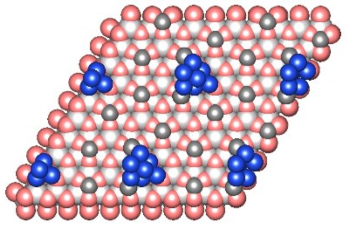	0.696185

O-poor O-terminated Surface

For the other O-poor reconstructed O-terminated surface (featuring O vacancies), a similar behaviour upon DFT refinement is observed, with the rough trend in relative stability being broadly reproduced (Table 10). Once again, the IP global minimum structure is also found to be the DFT global minimum, the difference in relative stability between the 1st and 2nd ranked IP structures is preserved upon DFT refinement, and the 3rd and 4th ranked IP structures are considerably less stable based on the DFT relative stability, compared to that obtained with IP methods. However, upon DFT refinement, the 5th ranked IP structure is found to be considerably lower in energy, such that is becomes the 2nd lowest energy DFT structure. Furthermore, whilst the 4th lowest energy IP structure is still determined to be much less stable than the global minimum upon DFT refinement, the DFT refined relative energies show that this structure is more stable than the 3rd ranked IP structure after DFT refinement is performed. Whilst the rationalisation of the differences between the IP and DFT refined structures is less clear in this case, it is evident that the lowest energy DFT structures (i.e. the 1st, 2nd and 5th ranked IP structures) all consist of a Cu cluster featuring a flat top surface with high Cu-Cu coordination, with the remainder of the Cu atoms being located underneath within the surface O vacancy pit. Moreover, the IP structures all feature much flatter Cu clusters with a greater proportion of Cu atoms being positioned fully within the O vacancy pit and lying beneath the surface defined by the topmost ZnO layer. This difference perhaps reflects an overestimation of the Cu-Zn interaction using the IP approach, which was suspected as a possible cause of the differences between the IP and DFT optimised structures for the O terminated surface with Zn adatoms. In any case, the IP global minimum structure was found to also be the DFT global minimum structure, therefore confirming the efficacy of the IP global optimisation approach as a reliable screening method for finding low-energy structures, even with the relatively small discrepancies arising from the limitations of the IP approach.

Table S6: *Structure and relative stability for the top 5 ranked low energy IP structures for Cu_8 clusters adsorbed on the reconstructed O-terminated ZnO surface featuring O vacancies, before and after DFT refinement.*

IP Rank	IP Structure	IP Relative E / eV	DFT Structure	DFT Relative E / eV
1	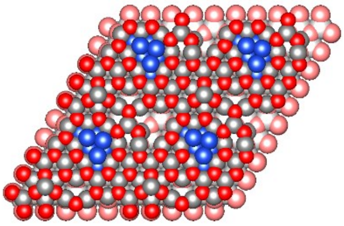	0.000000	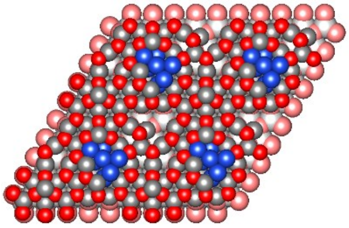	0.000000
2	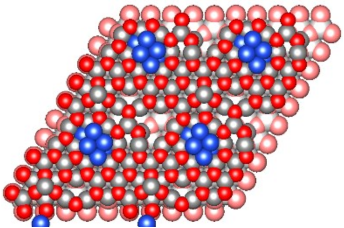	0.205843	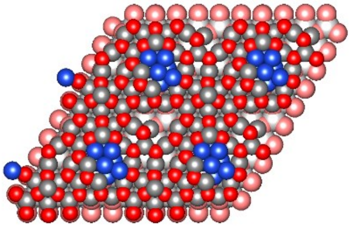	0.214580
3	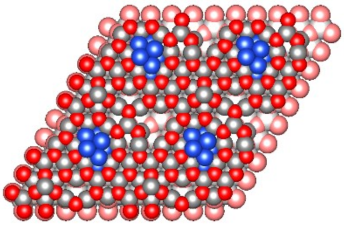	0.256887	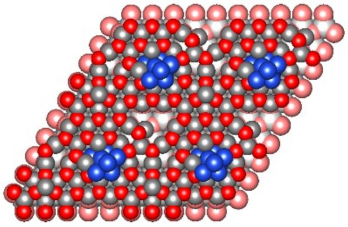	0.686893
4	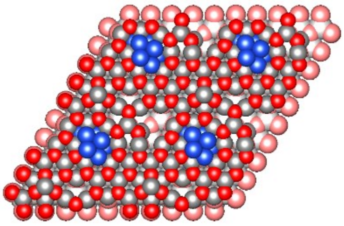	0.339511	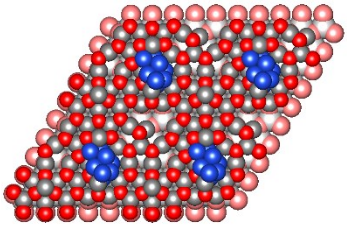	0.555472
5	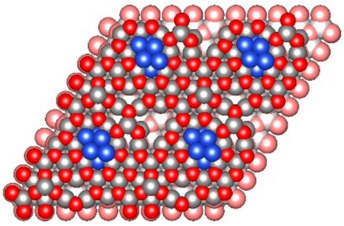	0.372239	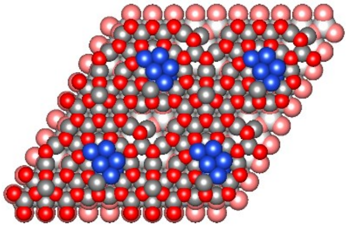	0.06003

O-rich Zn-terminated Surface

We turn now to the O-rich Zn-terminated reconstructed surface and the DFT refinement of the Cu_8 clusters adsorbed upon this surface. DFT refinement results in a significant deviation in terms of both Cu cluster structure, and relative stability (Table 11). Perhaps the two most striking structural features evident post-refinement are the close proximity of Cu and surface O adatoms, and the considerable displacement of these surface O adatoms with respect to their positions in the IP optimised structures; during IP optimisation, these atoms largely remain unperturbed from their positions on the clean IP optimised surfaces. These differences can be rationalised by considering the fact that the highly undercoordinated surface O adatoms are likely to be considerably less reduced compared to their bulk and subsurface counterparts, owing to having fewer Zn neighbours. Not only would this reduce the repulsive interaction between Cu and O implied by the potentials used (i.e. both species being comparatively electron rich), but also open the possibility for electron transfer from Cu to O (that is to say, partial Cu oxidation), which clearly cannot be accounted for explicitly using the IP approach but is taken into consideration using a DFT approach. In tandem, these two conclusions support the observed changes upon DFT refinement, which suggest a stronger and more attractive interaction between the surface O adatoms and the Cu cluster atoms.

The higher mobility of the surface O adatoms (which may be attributed both to a weaker O-Zn interaction and stronger Cu-O interaction for these surface O adatoms compared to that assumed by the IP approach) appears to play an important role in the re-ordering of the lowest energy structures upon DFT refinement. For the IP optimised Cu_8 clusters, the surface O adatoms present a barrier to the favoured planar Cu cluster growth across the flat Zn-terminated surface observed for smaller Cu clusters, hence the IP global minimum features a 3D Cu cluster (consisting of a highly coordinated Cu_7 planar base, with an additional Cu atom on top), whilst the remaining 4 lowest energy structures all feature flat Cu_8 clusters that compromise Cu-Cu coordination in order to minimise close contact with the O surface adatoms. However, upon DFT refinement, no such condition appears to be present, hence the DFT global minimum (which was obtained from refinement of the the 5th lowest energy IP structure) features a distinctive planar Cu cluster with a minimal perimeter (maximising Cu-Cu coordination), with the surface O adatoms positions at the corners of the flat Cu cluster (i.e. interacting with the least coordinated Cu atoms). By contrast, the IP global minimum structure is only the 4th lowest energy DFT structure (whilst retaining its 3D morphology), with only the 3rd lowest energy IP structure being found to be less stable upon DFT refinement, this being attributed to the low Cu-Cu coordination evident in the initial IP structure, which is preserved upon DFT optimisation.

Clearly, in this case, the IP global optimisation approach cannot be used alone to approximate DFT global minimum energy structures. However, the present results neatly illustrate the limitations of the approach and provide key insights that will be invaluable in the tailoring of the interatomic potentials to meet the needs of more complex systems.

Table S7: *Structure and relative stability for the top 5 ranked low energy IP structures for* Cu_8 *clusters adsorbed on the reconstructed Zn-terminated ZnO surface featuring O adatoms, before and after DFT refinement.*

IP Rank	IP Structure	IP Relative E / eV	DFT Structure	DFT Relative E / eV
1	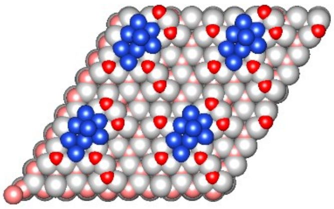	0.000000	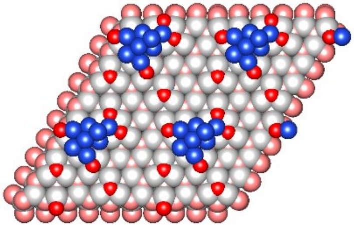	2.085816
2	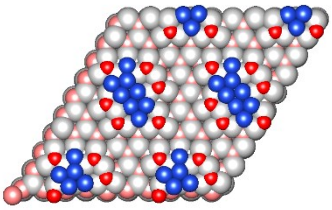	0.054160	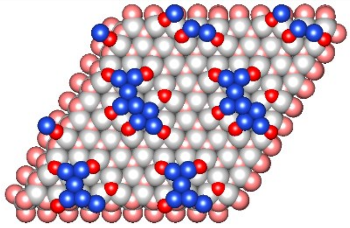	1.062999
3	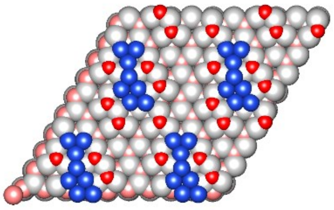	0.112844	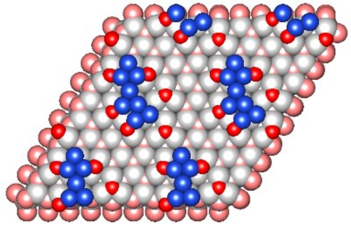	2.452742
4	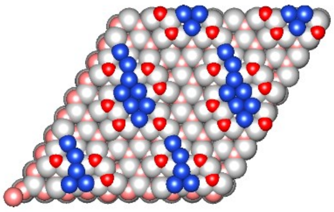	0.131735	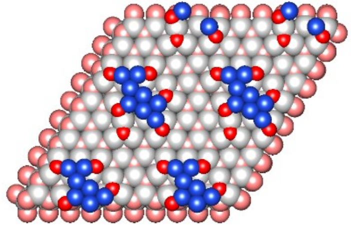	1.183166
5	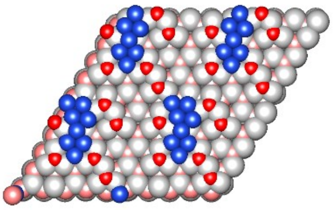	0.201058	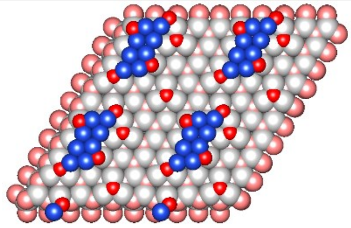	0.000000

Zn-poor Zn-terminated Surface

The final system to be considered for DFT refinement consists of Cu_8 clusters adsorbed on the Zn-poor Zn-terminated reconstructed polar surface (featuring Zn vacancies). Here, the DFT refined structures show a broad agreement with the IP optimised structures, in common with both of the O-terminated surfaces already discussed (Table 12). The lowest energy IP global minimum is found to also be the DFT optimised lowest energy structure. However, all of the remaining 4 lowest energy structures are found to be considerably less stable upon DFT refinement, with all of them being over ~1.3 eV less stable than the DFT global minimum structure. Whilst the ordering of the 1st and 2nd lowest energy IP structures is preserved upon DFT optimisation, the 3rd ranked IP structure is found to be considerably less stable upon DFT refinement, whereas the inverse is true for the 5th lowest energy IP structure, which is found to be the 3rd lowest energy DFT structure.

The enhanced stability of the DFT global minimum structure compared to its IP counterpart can be linked to the lesser degree of O reduction for the O atoms that define the Zn surface vacancy pit. Whilst the highly coordinated planar Cu_8 structure is largely retained upon DFT refinement of the IP global minimum, we see that the position of the cluster has shifted such that the least coordinated Cu atom (having only 2 Cu neighbours) is located within the Zn vacancy pit, implying a degree of Cu oxidation from interaction with the O atoms within the surface pit that lack a full complement of Zn neighbours. To test this, Bader charge analysis was performed; we find that the Cu atom located within the Zn vacancy surface pit is significantly more oxidised than the remaining 7 Cu atoms in the cluster, with a Bader charge increase of $\Delta\beta$=+0.57 e, with respect to a single isolated neutral Cu atom. By comparison, for the remaining 7 Cu atoms, $\Delta\beta$ ranges from +0.21 e to -0.06 e, averaging $\Delta\beta$=+0.09 e, consistent with essentially unoxidized Cu^0, with this small deviation being attributable to the charge delocalisation owing to the metallic character of Cu. The $\Delta\beta$ calculated for the Cu atom located within the Zn vacancy site is consistent with previous studies which determined the Bader charges for Cu and O in bulk Cu_2O, determining $\Delta\beta$=+0.53 e using the PBE GGA functional[36]. Hence, there is strong evidence that in the present system, the Cu atom which is located within the Zn surface vacancy site after DFT refinement corresponds to a Cu^+ cation, in line with previous DFT studies which suggest that oxidising Cu atoms within surface Zn vacancy sites can serve as anchor sites for Cu cluster growth[21]. This finding is consistent with our rationalisation of the more drastic changes observed for DFT refinement of the Cu clusters on top of the Zn-terminated surface featuring O adatoms. For the other DFT refined structures, no such migration of the Cu cluster to accommodate one Cu atom in a Zn vacancy site is observed, which is reflected in the gap in stability between the global minimum and all 4 of the remaining DFT optimised structures. Nonetheless, in all of the other structures, it is still the case that after DFT refinement, the Cu clusters adopt slightly more planar clusters; whilst none of the cluster geometries deviate significantly from their IP optimised positions atop the large hexagonal surface ZnO platform, the DFT refined structures show Cu atoms much closer to the edges of the hexagonal platform, decreasing the distance between the Cu atoms at the edge of the cluster and the undercoordinated O atoms defining the edges of the Zn vacancy pits. This result further suggests that the interaction between Cu and undercoordinated surface O is perhaps not as repulsive as that described using IP methods, agreeing with the rationalisation for the impact of DFT refinement on the Zn-terminated surface featuring O adatoms.

Table S8: *Structure and relative stability for the top 5 ranked low energy IP structures for* Cu_8 *clusters adsorbed on the reconstructed Zn-terminated ZnO surface featuring Zn vacancies, before and after DFT refinement.*

IP Rank	IP Structure	IP Relative E / eV	DFT Structure	DFT Relative E / eV
1	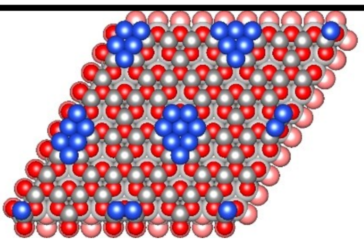	0.000000	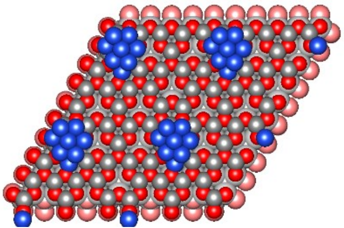	0.000000
2	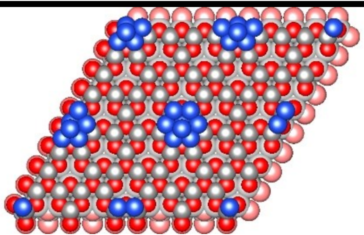	0.048902	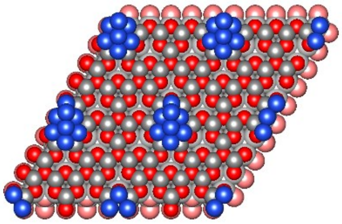	1.289726
3	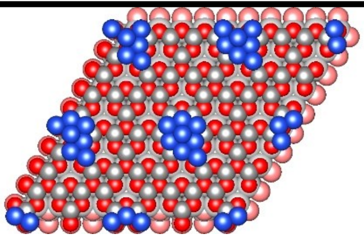	0.107006	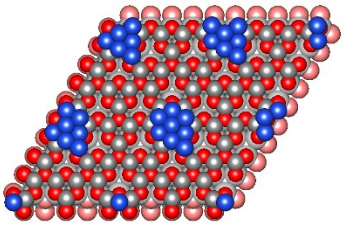	2.051926
4	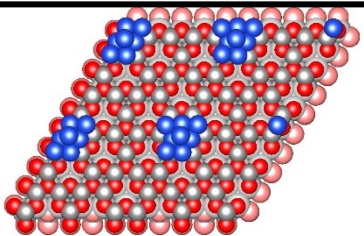	0.127718	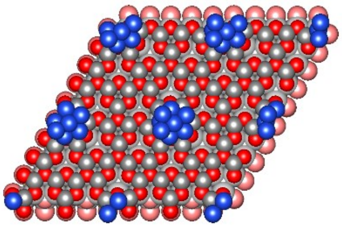	1.623505
5	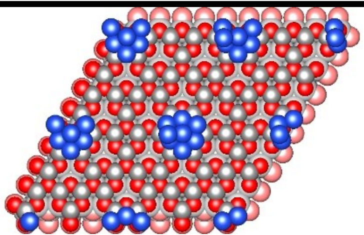	0.368287	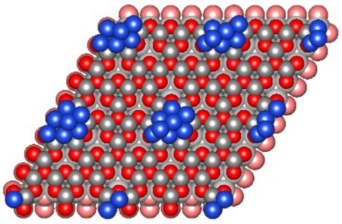	1.303548